Available online at www.sciencedirect.com
SCIENCE DIRECT®
Bioorganic & Medicinal Chemistry 12 (2004) 2537–2544
Bioorganic & Medicinal Chemistry

Synthesis, properties, and photodynamic properties in vitro of heavy-chalcogen analogues of tetramethylrosamine

Michael R. Detty,[a,*] Paras N. Prasad,[a] David J. Donnelly,[a] Tymish Ohulchanskyy,[a] Scott L. Gibson[b] and Russell Hilf[b]

[a]*Institute for Lasers, Photonics, and Biophotonics, Department of Chemistry, University at Buffalo, The State University of New York, Buffalo, NY 14260, USA*
[b]*Department of Biochemistry and Biophysics, University of Rochester Medical Center, 601 Elmwood Avenue, PO Box 607, Rochester, NY 14642, USA*

Received 26 January 2004; revised 1 March 2004; accepted 14 March 2004

Available online 13 April 2004

Abstract—Thio and seleno analogues of tetramethylrosamine were prepared by the directed-metalation/cyclization of the corresponding *N*,*N*-diethyl 2-(3-dimethylaminophenylchalcogeno)-4-dimethylaminobenzamide to the 2,7-bis-(*N*,*N*-dimethylamino)-9*H*-chalcogenoxanthen-9-one followed by the addition of phenylmagnesium bromide, dehydration, and ion exchange to the chloride salt. The thio and seleno tetramethylrosamines had longer wavelengths of absorption and higher quantum yields for the generation of singlet oxygen than tetramethylrosamine. Both the thio and selenoanalogues of tetramethylrosamine were efficient photosensitizers against R3230AC rat mammary adenocarcinoma cells in vitro.

1. Introduction

The xanthylium nucleus is the heart of many important chromophores in chemistry and biology. The rhodamine and rosamine dyes are representative of the xanthylium class and have been used as laser dyes, fluorescent labels, and fluorescence emission standards where their high fluorescence quantum yields and photostabilities are exploited.[1–5] The rhodamine dyes are also useful fluorescence probes in cell biology studies, showing specific fluorescence staining of mitochondria and other cell organelles.[6,7] The rhodamines have been found to accumulate selectively in carcinoma cells[8–10] and to be toxic to cancer cells both in vitro[10] and in vivo.[11]

One area where the xanthylium dyes have been minimally utilized is photodynamic therapy (PDT), where their tumor specificity might truly be exploited.[12,13] PDT is a treatment for various cancers that utilizes the combination of a tumor-specific photosensitizer, light, and molecular oxygen to induce cellular toxicity, presumably via the generation of singlet oxygen.[12] While rhodamine and rosamine dyes exhibit selective uptake in cancer cells, they are poor producers of excited-state triplets[14] and, consequently, of singlet oxygen. The poor triplet production limits the use of rhodamine and rosamine dyes as photosensitizers PDT. Furthermore, the rhodamines and rosamines absorb light of wavelengths too short for effective penetration in tissue.[12]

Heavy-atom effects in brominated rhodamine dyes give increased triplet yields and quantum yields for the generation of singlet oxygen [$\phi(^1O_2)$][15–17] relative to unmodified rhodamines.[18] However, wavelengths of absorption are little changed relative to their light-atom counterparts. The brominated analogues still target the mitochondria and have increased phototoxicity toward cancer cells.[17] We describe the synthesis of thio and seleno analogues of tetramethylrosamine (**TMR-S** and **TMR-Se**, respectively) where the heavy atom is part of the xanthylium chromophore. Not only does substitution of sulfur or selenium for oxygen give dramatic increases in the production of $^1O_2$, but this substitution also gives longer wavelengths of absorption and

Keywords: Photodynamic therapy; Anticancer drugs; Photosensitizers; Tetramethylrosamines; Thioxanthylium; Selenoxanthylium.
* Corresponding author. Tel.: +1-716-645-6800; fax: +1-716-645-6963; e-mail: mdetty@buffalo.edu

0968-0896/$ - see front matter © 2004 Elsevier Ltd. All rights reserved.
doi:10.1016/j.bmc.2004.03.029

emission and provides highly effective photosensitizers for PDT against R3230AC rat mammary adenocarcinoma cells in vitro.

2. Results and discussion

2.1. Synthesis

We have described the synthesis of 2,7-bis-*N*,*N*-dimethylamino-9*H*-selenoxanthen-4-one (**1**) from acyclic precursors via directed metalation reactions as shown in Scheme 1.[19] The same approach was used for the synthesis of 2,7-bis-*N*,*N*-dimethylamino-9*H*-thioxanthen-4-one (**2**). Lithiation of *N*,*N*-diethyl 4-dimethylaminobenzamide with *tert*-BuLi in the presence of *N*,*N*,*N*′,*N*′-tetramethylethylenediamine (TMEDA) followed by the addition of bis(3-dimethylaminophenyl)diselenide (**3**) or disulfide (**4**) gave *N*,*N*-diethyl-2-(3′-dimethylaminophenylseleno)-4-dimethylaminobenzamide (**5**) or 2-*N*,*N*-diethyl-2-(3′-dimethylaminophenylthio)-4-dimethylaminobenzamide (**6**) in 57% and 51% isolated yields, respectively. Cyclization of **5** and **6** with 2 equiv of lithium diisopropylamide (LDA) gave selenoxanthenone **1** in 23% yield and thioxanthenone **2** in 13% yield, respectively, with 70% recovered starting material in each case. The starting material could be recycled to give more **1** and **2**. Use of larger excesses of LDA gave up to 30% yields of **1** and **2**, but no starting material was recovered under these conditions.

The addition of phenylmagnesium bromide to chalcogenoxanthen-9-ones **1** and **2** followed by dehydration with HPF_6 gave 2,7-bis-*N*,*N*-dimethylamino-9-phenylselenoxanthylium and 2,7-bis-*N*,*N*-dimethylamino-9-phenylthioxanthylium hexafluorophosphates in 98% and 71% isolated yields, respectively. Anion exchange with Amberlite IRA-400 chloride exchange resin gave the corresponding chloride salts **TMR-Se**, and **TMR-S** in 78% and 75% isolated yields, respectively.

2.2. Photophysical properties

Various photophysical properties of **TMR-S** and **TMR-Se** are compared to those of commercially available tetramethylrosamine (**TMR-O**, Molecular Probes, Inc.) in Table 1. In MeOH, a 20-nm bathochromic shift for **TMR-S** and a 30-nm bathochromic shift for **TMR-Se** in the wavelength of the absorption maximum, λ_{max}, is observed as the chalcogen atom becomes larger and the oscillator strength of the band decreases as indicated by a decrease in the molar extinction coefficient, ε. Other series of chalcogenopyrylium dyes show similar trends.[20]

A 25–28 nm Stokes shift is observed in the fluorescence emission maximum, λ_F, which is typical of other cationic dyes.[20] The radiative lifetime, τ_{rad}, decreases from 2.1 ± 0.1 ns in **TMR-O** to 1.5 ± 0.1 ns for **TMR-S** to approximately 50 ps for **TMR-Se**, which is consistent with heavy-atom effects in other cationic dyes.[20]

The rigid nature of the xanthylium core minimizes internal conversion back to the ground state, which leads to dramatic changes in ϕ_F and $\phi(^1O_2)$ as the chalcogen atom becomes larger. Fluorescence in **TMR-O** is highly efficient with ϕ_Φ of 0.84. Intersystem crossing to the triplet, which is necessary for the production of singlet oxygen, is relatively slow with $\phi(^1O_2)$ of 0.08 for **TMR-O**. As the chalcogen atom becomes larger, the spin-orbit (heavy-atom) effects promote triplet formation relative to fluorescence and $\phi(^1O_2)$ decreases to 0.44 and 0.009 for **TMR-S** and **TMR-Se**, respectively, while

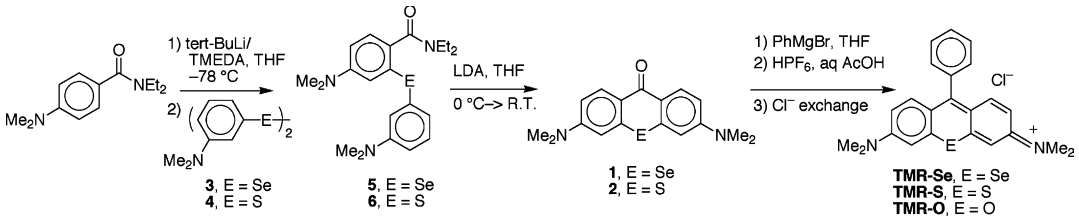

Scheme 1. Preparation of **TMR-Se** and **TMR-S**.

Table 1. Absorption (λ_{max}) and fluorescence (λ_F) maxima in MeOH, quantum yields for fluorescence (ϕ_F) and the generation of singlet oxygen [$\phi(^1O_2)$], reduction potentials ($E°$), and *n*-octanol/water partition co-efficients (log *P*) for **TMR-O**, **TMR-S**, and **TMR-Se**

Compound	λ_{max} (nm) (log ε)	λ_F (nm)[a]	$\phi_F \pm$ sd[b]	$\phi(^1O_2) \pm$ sd[c]	$E°$ (V)[d]	Log P[e]
TMR-O	552 (4.92)	575	0.84 ± 0.01	0.08 ± 0.01	−0.94	1.5
TMR-S	571 (4.70)	599	0.44 ± 0.01	0.21 ± 0.02	−0.79	1.2
TMR-Se	582 (4.84)	608	0.009 ± 0.001	0.87 ± 0.01	−0.77	1.1

[a] Excitation at 532 nm.
[b] Quantum efficiencies using rhodamine 6 G as a standard.
[c] Direct detection of singlet-oxygen luminescence using rose bengal as a standard.
[d] In CH_2Cl_2 with 0.2 N Bu_4NBF_4 as supporting electrolyte. V versus the ferrocene/ferrocinium couple ($E° = +0.40$ V).
[e] pH 6 Phosphate buffer as the aqueous phase.

values of $\phi(^1O_2)$ increase to 0.21 and 0.87 for **TMR-S** and **TMR-Se**, respectively.

2.3. Chemical properties

Mitochondrial reduction of a cationic photosensitizer can bleach the photosensitizer limiting the useful lifetime of the photosensitizer. Furthermore, the cationic photosensitizer's role as an electron acceptor might impact the redox cascade in mitochondrial respiration. The reduction potentials of **TMR-O**, **TMR-S**, and **TMR-Se** were determined by cyclic voltametry and values of $E°$ for the cation/neutral radical couple [vs the ferrocene/ferrocinium couple (Fc/Fc^+) at +0.40 V] are compiled in Table 1. An anodic (positive) shift in $E°$ is observed as the chalcogen atom becomes heavier. The reduction of the tetramethylrosamines is more cathodic (more difficult to reduce) than the thiopyrylium dye **AA1** [$E°$ of −0.71 V (vs Fc/Fc^+)], which shows antitumor activity by targeting the mitochondria of carcinoma cells[21] and inhibiting mitochondrial ATPase activity.[21]

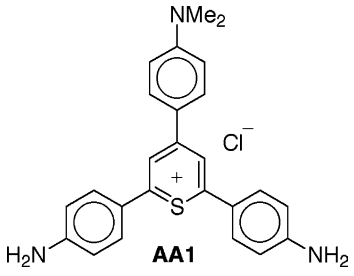

Values of the *n*-octanol/water partition coefficient ($\log P$) were determined for the tetramethylrosamine series using a pH 6 phosphate buffer[22] as the aqueous phase and are compiled in Table 1. Values of $\log P$ are somewhat smaller for the tetramethylrosamine series ($\log P$ of 1.1–1.5) relative to **AA1** ($\log P$ of 1.9), which might have some impact with respect to uptake and localization within the cell.

2.4. Biological studies. Dark and phototoxicity toward R3230AC cells

The tetramethylrosamine series was evaluated for dark and phototoxicity against R3230AC rat mammary adenocarcinoma cells. Cell cultures were incubated for 3 h in the dark with various concentrations of dye and were then washed prior to treatment with filtered 360–800 nm light from a tungsten–halogen source at 1.4 mW cm^{-2} for a total light dose up to 5.0 J cm^{-2}. Light-treated cells and dark controls were incubated for 24 h and cell survival was determined. At concentrations $\leqslant$1.0 μM, none of the tetramethylrosamine series showed any significant dark toxicity toward R3230AC cells relative to untreated dark controls ($P < 0.05$) and values of LD_{50}, the concentration necessary to give 50% cell kill in the dark with 3 h incubation, were >5μM for each dye.

TMR-O displayed no added phototoxicity that was statistically significant upon irradiation, which is consistent with results with other rhodamines. However, both **TMR-S** and **TMR-Se** were efficient photosensitizers toward R3230AC cells with phototoxicity increasing with dye concentration and constant light dose (Fig. 1a) or with constant dye concentration and increasing light dose (Fig. 1b). With 0.1 μM solutions of either **TMR-S** or **TMR-Se** and irradiation with 5.0 J cm^{-2} of 360–800 nm light, surviving fractions were less than 0.50 (Fig. 1a). Furthermore, statistically significant ($P < 0.05$) phototoxicity was also observed with 0.05 μM **TMR-S** and **TMR-Se** (Fig. 1a). For both **TMR-S** and **TMR-Se**, the therapeutic ratio LD_{50} divided by the effective concentration to kill 50% of the cells (EC_{50}, $\leqslant$0.1 μM for each) was >50.

2.4.1. Intracellular accumulation of TMR-O, TMR-S, and TMR-Se. The intracellular accumulation of **TMR-O** and **TMR-S** was determined in R3230AC cells incubated with 10 μM dye for 3 h. Longer incubation periods had little impact on final intracellular concentrations. Intracellular dye concentration was determined by

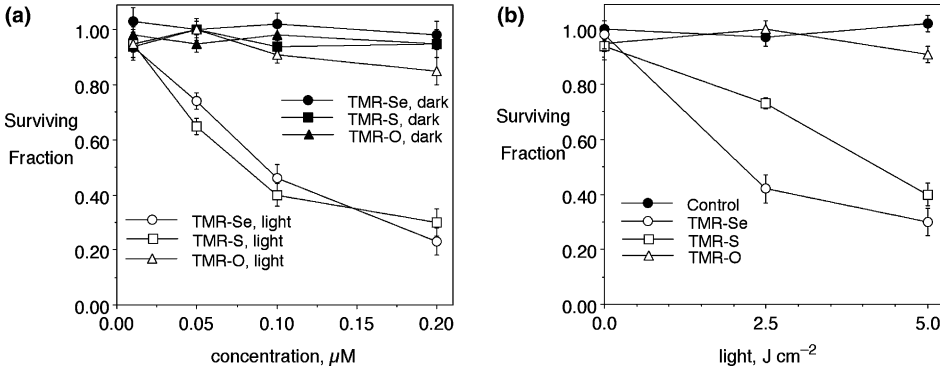

Figure 1. Effect of dyes **TMR-O**, **TMR-S**, and **TMR-Se** on the viability of R3230AC cells in culture in the dark or 24 h after exposure to (a) various concentrations of dye and 5.0 J/cm^2 of filtered 360–800 nm light or (b) 0.1 μM dye and variable light doses. Each point represents three separate experiments performed in duplicate for the viability of cultured R3230AC cells maintained in the dark or 24 h after exposure of cells to light. Data are expressed as the fraction of control cell viability, exposed to neither dyes nor light, error bars are the SEM.

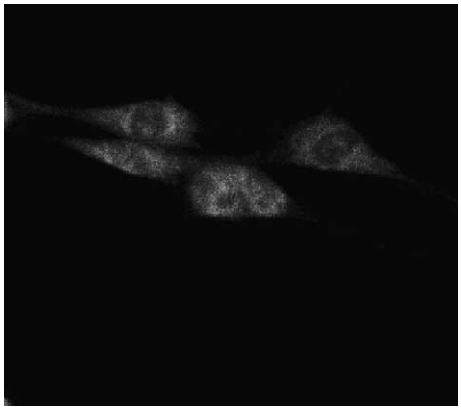

Figure 2. CSLM image of R3230AC cells treated with 2 μM **TMR-Se** for 1.5 h with excitation at 532 nm.

fluorescence in cell lysates and was 16 ± 3 fmol of dye per cell for **TMR-O** and 14 ± 2 fmol of dye per cell for **TMR-S**.

The fluorescence from cell lysates of **TMR-Se** treated cells was too weak to determine the intracellular dye concentration accurately. However, the cellular uptake of **TMR-Se** could be observed by confocal scanning laser microscopy (CSLM). R3230AC cells were incubated for 1.5 h with 2 μM **TMR-Se** in culture media and were then washed and covered with fresh media. The CSLM fluorescence micrographs of these cells show a diffuse fluorescence from **TMR-Se** within the cell with minimal staining of the nucleus (Fig. 2).

3. Conclusions

The rhodamines and related structures have interesting biological properties that included selective localization in the mitochondria of carcinoma cells.[8–10] At high concentrations, these materials can show antitumor activity.[10,11] Unfortunately, the rhodamines have had limited use in PDT since these molecules absorb only wavelengths of light that do not penetrate tissues effectively and show no added phototoxicity upon irradiation unless heavy atoms are incorporated into their structure. While brominated rhodamines function as photosensitizers, their wavelengths of absorption are unchanged by this substitution.[16,17] Highly efficient photosensitizers for photodynamic therapy can be obtained by substituting the heavier chalcogen atoms sulfur and selenium for the oxygen atom in these molecules. Both **TMR-S** and **TMR-Se** absorb longer wavelengths of light and generate singlet oxygen much more efficiently upon irradiation than **TMR-O**.

In R3230AC rat mammary adenocarcinoma cells, values of EC_{50} for both **TMR-S** and **TMR-Se** are <0.1 μM with 5.0 J cm^{-2} of filtered 360–800 nm light while the LD_{50} of dark controls is >5 μM. These in vitro studies have a therapeutic ratio of >50. Fluorescence studies indicated that the uptake of **TMR-S** and **TMR-O** was nearly identical, which suggests that the phototoxicity associated with **TMR-S** is the result of improved photophysical properties. While we could not quantify the cellular uptake of **TMR-Se**, confocal microscopy studies confirmed the uptake of **TMR-Se** by the R3230AC cells. Continuing studies will focus on the subcellular localization of **TMR-S** and **TMR-Se** as well as the performance of **TMR-S**, and **TMR-Se** in vivo.

4. Experimental

4.1. General methods

Solvents and reagents were used as received from Sigma–Aldrich Chemical Co. (St. Louis, MO) unless otherwise noted. Tetramethylrosamine (**TMR-O**) was purchased from Molecular Probes, Inc. Cell culture media and antibiotics were obtained from Grand Island Biological (Grand Island, NY). Fetal bovine serum (FBS) was purchased from Atlanta Biologicals (Atlanta, GA). Concentration in vacuo was performed on a Büchi rotary evaporator. Chalcogenoxanthones **1** and **2** were prepared according to Ref. 19. NMR spectra were recorded on a Varian Inova 500 instrument with residual solvent signal as internal standard. UV–vis-near-IR spectra were recorded on a Perkin–Elmer Lambda 12 spectrophotometer equipped with a circulating constant-temperature bath for the sample chambers. Elemental analyzes were conducted by Atlantic Microlabs, Inc.

4.1.1. Preparation of bis(3-dimethylaminophenyl)disulfide (4). 3-Bromo-*N*,*N*-dimethylaniline (1.0 g, 5.0 mmol) was added to a stirred mixture of Mg turnings (0.243 g, 10.0 mmol) in 10 mL of anhydrous THF. The resulting mixture was heated reflux for 2 h and then cooled to ambient temperature. Sulfur powder (0.39 g, 5.0 mmol) was added and the resulting mixture was heated at reflux for 2 h. The reaction mixture was cooled to ambient temperature and then poured over 6 g of ice. HCl (10 mL, 5%) was added and the resulting mixture was filtered through a pad of Celite. The crude thiol was oxidized via the addition of 0.074 g (0.24 mmol) of dihexyltelluride and 10 mL of 30% H_2O_2.[23] After stirring for 1 h, the reaction mixture was poured into 50 mL of water and the crude product was extracted with ether (3×25 mL). The combined organic extracts were washed with brine, dried over $MgSO_4$, and concentrated. The crude oil was purified via chromatography on SiO_2 eluted with 10% cyclohexane/CH_2Cl_2 to give 0.79 g (52%) of the disulfide **4** as a white powder, mp 91–92 °C: ^{1}H NMR (CD_2Cl_2) δ 7.81 (d, 2H, $J = 6.7$ Hz), 7.21 (d × d, 1H, $J = 2.0$, 6.7 Hz), 3.35 (s, 12 H); HRMS (EI), m/z 304.1065 (calcd for $C_{16}H_{20}N_2S_2$: 304.1068). Anal. Calcd for $C_{16}H_{20}N_2S_2$: C, 63.12; H, 6.62; N, 9.20. Found: C, 63.08; H, 6.62; N, 9.23.

4.1.2. Preparation of *N*,*N*-diethyl-2-(3′-dimethylaminophenylthio)-4-dimethylaminobenzamide (6). *sec*-Butyl-

lithium (1.3 M in cyclohexane, 2.7 mL, 3.6 mmol) was added dropwise to a stirred solution of *N*,*N*-diethyl 4-*N*,*N*-dimethylamino benzamide (0.79 g, 3.6 mmol) and *N*,*N*,*N*,*N*-tetramethylethylenediamine (TMEDA, 0.42 g, 3.6 mmol) in 25 mL of anhydrous THF at −78 °C. After 1 h at −78 °C, disulfide **4** (1.43 g, 3.6 mmol) in 5 mL of THF was added dropwise. After 0.5 h at −78 °C, the reaction mixture was warmed to ambient temperature. Saturated NH_4Cl (10 mL) was added and the products were extracted with CH_2Cl_2 (3 × 30 mL). The combined organic extracts were washed with brine, dried over $MgSO_4$, and concentrated. The crude product was purified via chromatography on SiO_2 eluted with 20% ether/CH_2Cl_2 to give 0.25 g (51%) of **6** as a pale yellow oil: ^{1}H NMR (CD_2Cl_2) δ 7.17 (t, 1H, $J = 8$ Hz), 7.08 (d, 1H, $J = 8.5$ Hz), 6.81 (t, 2H, $J = 2$ Hz), 6.69 (d, 1H, $J = 8$ Hz), 6.63 (dd, 1H, $J = 2$, 8.5 Hz), 6.60 (d, 1H, $J = 2$ Hz), 6.58 (d × d, 1H, $J = 2$, 8.5 Hz); 3.50 (exchange br s, 4 H), 3.18 (s, 6 H), 2.86 (exchange br s, 6H); ^{13}C NMR (CD_2Cl_2) δ 169.5, 151.4, 151.0, 135.7, 133.8, 129.7, 127.5, 127.2, 119.7, 115.6, 115.0, 111.6, 111.0, 43.2 (br), 40.5, 40.2, 14.2 (br); IR (film, NaCl) 1621, 1594 cm^{-1}; HRMS (ES) *m*/*z* 372.2109 (calcd for $C_{21}H_{30}N_3OS + H$: 372.2104).

4.1.3. Preparation of 2,7-bis-*N*,*N*-(dimethylamino)thioxanthen-9-one (2). To a solution of **6** (0.52 g, 1.5 mmol) in 10 mL of THF at 25 °C was added LDA (1.0 M in hexanes, 3.6 mL, 3.6 mmol). The resulting mixture was stirred at ambient temperature for 15 h and was quenched by the addition of 20 mL of saturated NH_4Cl. The products were extracted with CH_2Cl_2 (3 × 10 mL) and the combined organic extracts were washed with brine, dried over Na_2SO_4, and concentrated. The products were purified via chromatography on SiO_2 eluted with 10% ether/CH_2Cl_2 to give 0.37 g (70%) of recovered **6** and 0.52 g (13%) of **2** as a yellow powder, mp 260–261 °C: ^{1}H NMR (500 MHz, CD_2Cl_2) δ 8.33 (d, 2H, $J = 9.2$ Hz), 6.80 (d × d, 2H, $J = 2.1$, 9.2 Hz), 6.77 (d, 2H, $J = 2.1$ Hz), 3.07 (s, 12H); ^{13}C NMR (CD_2Cl_2) 177.2; 151.7, 138.6, 130.2, 118.5, 110.9, 104.8, 39.6; IR (KBr) 1592 cm^{-1}; HRMS (ES) *m*/*z* 299.1217 (calcd for $C_{17}H_{18}ON_2$ S + H: 299.1213).

4.1.4. Preparation of 2,7-bis-*N*,*N*-dimethylamino-9-phenylselenoxanthylium chloride (TMR-Se). A solution of 2,7-bis-*N*,*N*-dimethylamino-9*H*-selenoxanthen-9-one (**1**, 0.070 g, 0.20 mmol) in THF (3 mL) was added dropwise to a solution of phenylmagnesium bromide (1.0 mL of a 1.0 M solution in THF, 1.0 mmol) in THF (2 mL) heated to reflux. After addition was complete, the resulting solution was heated at reflux for an additional 0.5 h. The reaction mixture was then cooled to ambient temperature and poured into acetic acid (3.0 mL). Hexafluorophosphoric acid (60% weight solution in water) was added dropwise until the initial deep blue solution turned reddish yellow. Water (50 mL) was added and the resulting mixture was cooled at −10 °C precipitating the selenoxanthylium hexafluorophosphate salt. The dye was collected by filtration and the solid was washed with water (2 × 5 mL) and diethyl ether (2 × 5 mL). The crude product was recrystallized by dissolving the solid in 2 mL of hot CH_3CN, cooling to ambient temperature, slowly adding 2 mL of ether, and chilling. The recrystallized product was collected by filtration, washed with ether (2 × 5 mL), and dried to give 0.109 g (98%) of the hexafluorophosphate salt as a dark green solid: mp >260 °C; ^{1}H NMR (500 MHz, CD_2Cl_2) δ 7.62 (m, 3H), 7.44 (d, 2H, $J = 9.8$ Hz), 7.30 (m, 2H), 7.27 (d, 2H, $J = 2.5$ Hz), 6.83 (d × d, 2H, $J = 2.5$, 9.8 Hz), 3.25 (s, 12H); ^{13}C NMR (500 MHz, CD_2Cl_2) δ 161.3, 152.6, 146.1, 138.1, 136.9, 128.9, 128.8, 128.3, 119.6, 114.4, 109.2, 40.4; λ_{max} (CH_2Cl_2) 582 nm ($\varepsilon = 6.9 \times 10^4$ M^{-1} cm^{-1}); HRMS (ES) *m*/*z* 407.1038 (calcd for $C_{23}H_{23}N_2^{80}Se$: 407.1026). Anal. Calcd for $C_{23}H_{23}F_6N_2OPSe$: C, 50.10; H, 4.20; N, 5.08. Found: C, 50.20; H, 4.32; N, 4.96.

The hexafluorophosphate salt (0.109 g, 0.068 mmol) was dissolved in 20 mL of acetonitrile and 0.500 g of Amberlite IRA-400 chloride ion exchange resin was added. The resulting mixture was stirred 0.5 h, the exchange resin was removed via filtration, and the process was repeated with two additional 0.500 g aliquots of the ion exchange resin. Following the final ion exchange, the filtrate was concentrated and the solid residue was recrystallized from acetonitrile, and a small amount of diethyl ether to give 0.081 g (75%) of 2,7-bis-*N*,*N*-dimethylamino-9-phenylselenoxanthylium chloride (**TMR-Se**) as a dark purple solid: mp >260 °C; ^{1}H NMR (500 MHz, CD_2Cl_2) δ 7.63 (m, 3H), 7.44 (d, 2H, $J = 6.1$), 7.30 (d × d, 2H, $J = 1.8$, 7.3 Hz), 7.28 (d × d, 2H, $J = 2.1$, 7.3 Hz), 6.83 (d × d, 2H, $J = 2.1$, 9.1 Hz), 3.25 (s, 12H); λ_{max} (H_2O) 580 nm ($\varepsilon = 5.9 \times 10^4$ M^{-1} cm^{-1}); HRMS (ES) *m*/*z* 407.1038 (calcd for $C_{23}H_{23}N_2^{80}Se$: 407.1026). Anal. Calcd for $C_{23}H_{23}ClN_2OSe$: C, 62.52; H, 5.25; N, 6.34. Found: C, 62.46; H, 5.08; N, 6.28.

The incorporation of selenium into the xanthylium core is clearly shown in Figure 3 where the parent ion cluster for **TMR-Se** is consistent with the theoretical spectrum for $C_{23}H_{23}N_2Se$.

4.1.5. Preparation of 2,7-bis-*N*,*N*-dimethylamino-9-phenylthioxanthylium chloride (TMR-S). A solution of 2,7-bis-*N*,*N*-dimethylamino-9*H*-thioxanthen-9-one (**2**, 0.050 g, 0.17 mmol) in THF (3 mL) was treated with phenylmagnesium bromide (1.0 mL of a 1.0 M solution in THF, 1.0 mmol) in THF (2 mL) as described for **TMR-Se**. Workup and recrystallization gave 0.078 g (71%) of 2,7-bis-*N*,*N*-dimethylamino-9-phenylthioxanthylium hexafluorophosphate: mp >260 °C; ^{1}H NMR (500 MHz, CD_2Cl_2) δ 7.68 (m, 3H), 7.47 (d, 2H, $J = 9.8$ Hz), 7.37 (m, 2H), 7.14 (d, 2H, $J = 2.4$ Hz), 6.95 (d × d, 2H, $J = 2.4$, 9.8 Hz), 3.31 (s, 12H); ^{13}C NMR (500 MHz, CD_2Cl_2) δ 153.5, 144.4, 136.5, 135.4, 129.5, 129.2, 128.7, 119.2, 115.1, 114.2, 105.4, 40.5; λ_{max} (CH_2Cl_2) 571 nm ($\varepsilon = 5.0 \times 10^4$ M^{-1} cm^{-1}); HRMS (ESI) *m*/*z* 359.1580 (calcd for $C_{23}H_{23}N_2S$: 359.1582). Anal. Calcd for $C_{23}H_{23}F_6N_2OPS$: C, 54.76; H, 4.60; N, 5.55. Found: C, 54.75; H, 4.75; N, 5.24.

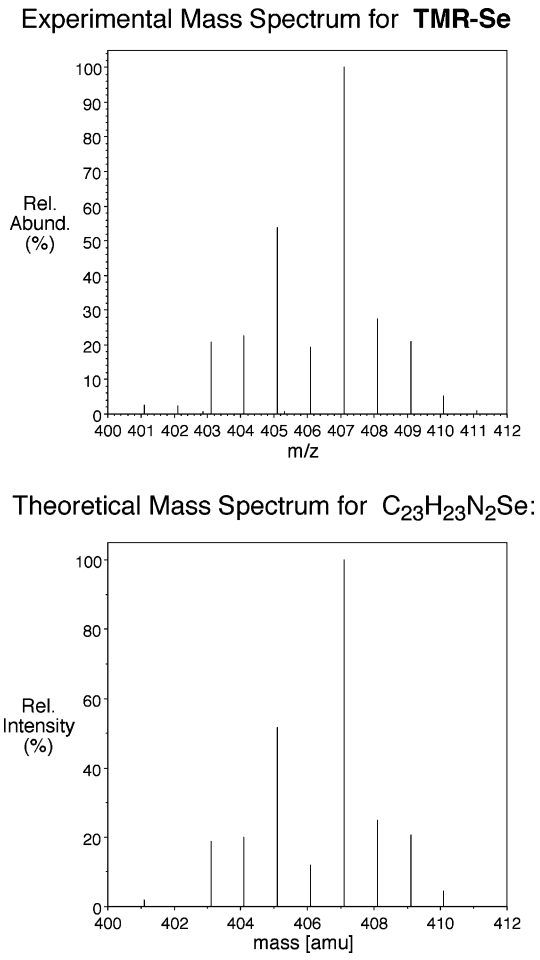

Figure 3. A comparison of the experimental mass spectrum of **TMR-Se** (top) with the theoretical mass spectrum of a molecule with the formula $C_{23}H_{23}N_2Se$ (bottom).

The hexafluorophosphate salt (0.045 g, 0.068 mmol) was treated with Amberlite IRA-400 chloride ion exchange resin as described for the preparation of **TMR-Se** to give 0.026 g (78%) of 2,7-bis-*N*,*N*-dimethylamino-9-phenylthioxanthylium chloride (**TMR-S**) as a dark green, crystalline solid: mp >260 °C; ^{1}H NMR (500 MHz, CD_2Cl_2) δ 7.67 (m, 3H), 7.46 (d, 2H, $J = 9.1$ Hz), 7.36 (m, 2H), 7.14 (d, 2H, $J = 2.5$ Hz), 6.95 (d × d, 2H, $J = 2.5$, 9.1 Hz), 3.31 (s, 12H); λ_{max} (H_2O) 570 nm ($\varepsilon = 4.0 \times 10^4$ M^{-1} cm^{-1}); HRMS (ESI), m/z 359.1579 (calcd for $C_{23}H_{23}N_2S$: 359.1582). Anal. Calcd for $C_{23}H_{23}ClN_2OS$: C, 69.94; H, 5.87; N, 7.07. Found: C, 70.03; H, 5.75; N, 7.05.

4.2. Quantum yield determinations for the generation of singlet oxygen

The quantum yields for singlet-oxygen generation with chalcogenoxanthylium dyes **TMR-O**, **TMR-S**, **TMR-Se**, and **6-Se** were measured by direct methods in MeOH.[24] A SPEX 270M spectrometer (Jobin Yvon) equipped with InGaAs photodetector (Electro-Optical Systems Inc., USA) was used for recording singlet-oxygen emission spectra. A diode pumped solid-state laser (Millenia X, Spectra-Physics) at 532 nm was the excitation source. The sample solution in a quartz cuvette was placed directly in front of the entrance slit of the spectrometer and the emission signal was collected at 90° relative to the exciting laser beam. An additional long-pass filter (850LP) was used to attenuate the excitation laser and the fluorescence from the photosensitizer.

4.3. Fluorescence quantum yields and radiative lifetimes

Fluorescence quantum yields (ϕ_F) and radiative lifetimes (τ_{rad}) were determined using techniques and equipment that we have previously described.[25]

4.4. Electrochemical procedures

A BAS 100 potentiostat/galvanostat and programmer were used for the electrochemical measurements. The working electrode for cyclic voltammetry was a platinum disk electrode (1 mm diameter) obtained from Princeton Applied Research. The auxiliary and reference electrodes were silver wires. The reference for cyclic voltammetry was the ferrocene/ferrrocinium couple at +0.40 V at a scan rate of 0.1 V s^{-1}. All samples were run in J. T. Baker HPLC-grade dichloromethane that had been stored over 3 Å molecular sieves and freshly distilled prior to use. Tetrabutylammonium fluoroborate (Sigma–Aldrich) was recrystallized from EtOAc–ether and then dried overnight at 80 °C under vacuum before it was used as supporting electrolyte at 0.2 M. Nitrogen was used for sample deaeration.

4.5. Determination of partition co-efficients

The octanol/water partition co-efficients were all measured at pH 6 (phosphate-buffered) using UV–vis spectrophotometry. The measurements were done using a 'shake flask' direct measurement.[26] Mixing for 3–5 min was followed by 1 h of settling time. Equilibration and measurements were made at 23 °C using a Perkin–Elmer Lambda 12 spectrophotometer. HPLC grade 1-octanol was obtained from Sigma–Aldrich.

4.6. Cells and culture conditions

R3230AC, a rat mammary adenocarcinoma line,[27,28] was maintained in a growth medium of minimum essential media (α-MEM) supplemented with 10% bovine serum albumin (FBS, Atlanta Biologicals, Atlanta, GA), 50 units/mL of penicillin G, 50 mg/mL of streptomycin, and 1.0 mg/mL of Fungizone.

4.7. Irradiation of cultured R3230AC cells

After seeding on 12-well plates, R3230AC cells were incubated for 24 h to allow cells to attach to the surface. Stock solutions of **TMR-O**, **TMR-S**, or **TMR-Se**, prepared at 1×10^{-3} M, were then added directly to the cell

culture medium to give a final dye concentration of 0.01–10 μM. Cell monolayers were then incubated for 3 h at 37 °C in the dark in a humidified 5% CO_2 atmosphere. The media was then removed and 1.0 mL of α-MEM minus FBS and phenol red (clear medium) was added to each well. One plate, with the lid removed, was then exposed to 360–800 nm light delivered at 1.4 mW cm^{-2} for 1 h (5.0 J cm^{-2}) from a filtered tungsten source for dye concentrations $\leqslant$0.1 μM. The remaining plate was kept in the dark during the irradiation period. Immediately following irradiation the clear medium was replaced with complete medium and the monolayers were incubated for an additional 24 h period as above. Subsequently, cells were trypsinized and counted to determine cell viability.

4.8. Measurement of dye uptake into cell monolayers

Twenty-four hours after seeding R3230AC cells on 12-well plates, **TMR-Se**, **TMR-S**, or **TMR-O** were added at 10 μM in α-MEM plus FBS and phenol red. Cells were incubated for 3 h in the presence of each dye in a humidified atmosphere in the dark as described above. The medium was then removed and the monolayers washed once with 1.0 mL of 0.9% NaCl and 1.0 mL of 50% EtOH/1% glacial acetic acid was added. Cells detached from the surface within 5 min and the dye emission in the resulting cell lysates was determined. Intracellular dye concentration was calculated by comparing emission values obtained from cell lysates with standard curves generated from known concentrations of dyes dissolved in a mixture of 50% EtOH/1% glacial acetic acid. Intracellular dye concentration is expressed in femtomole dye per cell.

4.9. Confocal laser scanning microscopy studies

R3230AC cells in 60-mm culture plates were treated with 5 mL of MEM alpha medium (without phenol red) containing 2 μM **TMR-Se**. The plates were returned to the incubator (37 °C, 5% CO_2) for a duration of 2 h. After incubation, the plates were rinsed with sterile PBS, and fresh media (without phenol red) was replaced at a volume of 5 mL/plate. The plates were then observed directly under the confocal microscope.

Confocal laser scanning microscopy images were obtained using a commercial confocal laser scanning microscope system (CLSM), model MRC-1024 (Bio-Rad, Richmond, CA), which was attached onto an upright microscope (Nikon, model Eclipse E800). A water immersion objective lens (Nikon, Fluor-60X, NA = 1.0) was used for cell imaging. A solid-state diode-pumped laser (Verdi, Coherent) was used as a source of excitation (532 nm). An additional long-pass filter (585LP) was introduced in front of the photomultiplier to minimize leakage of the excitation light. To confirm that the observed fluorescence was from photosensitizer permeated to cells, we used localized spectrofluorometry. The fluorescence signal was collected from the upper port of the confocal microscope using a multi-mode optical fiber of core diameter 1 mm, and was delivered to a spectrometer (Holospec from Kaiser Optical Systems, Inc.) equipped with a cooled charge coupled device (CCD) camera (Princeton Instruments) as detector. A comparison of the fluorescence spectra from cells and the fluorescence spectra of the photosensitizers confirmed that the origin of the fluorescence observed in the image channel was from the photosensitizer. Control cells showed no fluorescence under the same imaging conditions in the absence of photosensitizer.

4.10. Statistical analysis

Pairwise inter-comparisons among the experimental groups and comparisons with the controls were performed using the students' t test. A value of $P < 0.05$ is considered significant.

Acknowledgements

This work was done under research grants to M.R.D. from the NIH (Grant CA69155) and to P.N.P. from the Directorate of Chemistry and Life Sciences of the Air Force Office of Scientific Research through Defense University Research Initiatives on Nanotechnology (Grant F496200110358).

References and notes

1. Peterson, O. G.; Tuccio, S. A.; Snavely, B. B. *Appl. Phys. Lett.* **1970**, *17*, 245.
2. Ali, M.; Moghaddasi, J.; Ahmed, S. A. *J. Appl. Opt.* **1990**, *29*, 3945.
3. Karstens, T.; Kobs, K. *J. Phys. Chem.* **1980**, *84*, 1871.
4. Preininger, C.; Mohr, G. J.; Klimant, I.; Wolfbeis, O. S. *Anal. Chim. Acta* **1996**, *334*, 113.
5. Liu, J.; Diwu, Z.; Leung, W.-Y.; Lu, Y.; Patch, B.; Haugland, R. P. *Tetrahedron Lett.* **2003**, *44*, 43555.
6. Johnson, L. V.; Walsh, M. L.; Bockus, B. J.; Chen, L. B. *J. Cell Biol.* **1981**, *88*, 526.
7. Shea, C. R.; Sherwood, M. E.; Flotte, T. J.; Chen, N.; Scholz, M.; Hasan, T. *Cancer Res.* **1990**, *50*, 4167.
8. Summerhayes, I. C.; Lampidis, T. J.; Bernal, S. D.; Nadakavukaren, J. J.; Nadakavukaren, K. K.; Shepard, E. L.; Chen, L. B. *Proc. Natl. Acad. Sci. U.S.A.* **1982**, *79*, 5292.
9. Davis, S.; Weiss, M. J.; Wong, J. R.; Lampidis, T. J.; Chen, L. B. *J. Biol. Chem.* **1985**, *260*, 13844.
10. Lampidis, T. J.; Bernal, S. D.; Summerhayes, I. C.; Chen, L. B. *Ann. N.Y. Acad. Sci.* **1982**, *395*, 299.
11. Bernal, S. D.; Lampidis, T. J.; McIsaac, R. M.; Chen, L. B. *Science* **1986**, *222*, 169.
12. Dougherty, T. J.; Gomer, C. J.; Henderson, B. W.; Jori, G.; Kessel, D.; Korbelik, M.; Moan, J.; Peng, Q. *J. Natl. Cancer Inst.* **1998**, *90*, 889.
13. Shea, C. R.; Chen, N.; Wimberly, J.; Hasan, T. *Cancer Res.* **1989**, *49*, 3961.
14. Menzel, R.; Thiel, E. *Chem. Phys. Lett.* **1998**, *291*, 237.
15. Kessel, D.; Woodburn, K. *Br. J. Cancer* **1995**, *71*, 306–310.
16. Pal, P.; Zeng, H.; Durocher, G.; Girard, D.; Li, T. C.; Gupta, A. K.; Giasson, R.; Blanchard, L.; Gaboury, L.;

Balassy, A.; Turmel, C.; Laperriere, A.; Villeneuve, L. *Photochem. Photobiol.* **1996**, *63*, 161.
17. Villeneuve, L.; Pal, P.; Durocher, G.; Migneault, D.; Girard, D.; Giasson, R.; Balassy, A.; Blanchard, L.; Gaboury, L. *J. Fluoresc.* **1996**, *6*, 209.
18. Stracke, F.; Heupel, M.; Thiel, E. *J. Photochem. Photobiol. A* **1999**, *126*, 51.
19. Brennan, N. K.; Donnelly, D. J.; Detty, M. R. *J. Org. Chem.* **2003**, *68*, 3344.
20. Detty, M. R.; Merkel, P. B. *J. Amer. Chem. Soc.* **1990**, *112*, 3845.
21. Sun, X.; Wong, J. R.; Song, K.; Hu, J.; Garlid, K. D.; Chen, L. B. *Cancer Res.* **1994**, *54*, 1465.
22. Brennan, N. K.; Hall, J. P.; Davies, S. R.; Gollnick, S. O.; Oseroff, A. R.; Gibson, S. L.; Hilf, R.; Detty, M. R. *J. Med. Chem.* **2002**, *45*, 5123.
23. You, Y.; Ahsan, K.; Detty, M. R. *J. Amer. Chem. Soc.* **2003**, *125*, 4918.
24. Pandey, R. K.; Sumlin, A. B.; Constantine, S.; Aoudia, M.; Potter, W. R.; Bellnier, D. A.; Henderson, B. W.; Rodgers, M. A.; Smith, K. M.; Dougherty, T. J. *Photochem. Photobiol.* **1996**, *64*, 194.
25. Baker, G. A.; Bright, F. V.; Detty, M. R.; Pandey, S.; Stilts, C. E.; Yao, H. R. *J. Porphyrins Phthalocyanines* **2000**, *4*, 669.
26. Sangster, J. In *Octanol–Water Partition Co-efficients: Fundamentals and Physical Chemistry*; Fogg, P. G. T., Ed.; John Wiley and Sons: New York, 1997.
27. Hilf, R.; Michel, I.; Bell, C.; Freeman, J. J.; Borman, A. *Cancer Res.* **1965**, *25*, 286.
28. Hissin, P. J.; Hilf, R. *Cancer Res.* **1978**, *38*, 3646.